

In-beam γ -ray spectroscopy of very neutron-rich nuclei: Excited states in ^{46}S and ^{48}Ar

A. Gade,^{1,2} P. Adrich,¹ D. Bazin,¹ B. A. Brown,^{1,2} J. M. Cook,^{1,2} C. Aa. Diget,¹ T. Glasmacher,^{1,2} S. McDaniel,^{1,2} A. Ratkiewicz,^{1,2} K. Siwek,^{1,2} and D. Weisshaar¹

¹National Superconducting Cyclotron Laboratory, Michigan State University, East Lansing, Michigan 48824

²Department of Physics and Astronomy, Michigan State University, East Lansing, Michigan 48824

(Dated: November 13, 2018)

We report on the first in-beam γ -ray spectroscopy study of the very neutron-rich nucleus ^{46}S . The $N = 30$ isotones ^{46}S and ^{48}Ar were produced in a novel way in two steps that both necessarily involve nucleon exchange and neutron pickup reactions, $^9\text{Be}(^{48}\text{Ca}, ^{48}\text{K})\text{X}$ followed by $^9\text{Be}(^{48}\text{K}, ^{48}\text{Ar}+\gamma)\text{X}$ at 85.7 MeV/u mid-target energy and $^9\text{Be}(^{48}\text{Ca}, ^{46}\text{Cl})\text{X}$ followed by $^9\text{Be}(^{46}\text{Cl}, ^{46}\text{S}+\gamma)\text{X}$ at 87.0 MeV/u mid-target energy, respectively. The results are compared to large-scale shell-model calculations in the *sdpf* shell using the SDPF-NR effective interaction and Z -dependent modifications.

The quest to comprehend the structure of the atomic nucleus in the regime of large neutron excess is driving experimental and theoretical research programs worldwide. Modifications to the familiar ordering of single-particle orbits or new phenomena like the development of neutron halos have been observed in experiments and their microscopic description challenges theories that quantify the nuclear many-body system at large proton-neutron asymmetry.

The experimental challenges are (i) the production of these short-lived, radioactive nuclei and (ii) the study of their properties. Neutron-rich nuclei lighter than calcium are efficiently produced in-flight by the fragmentation of a stable ^{48}Ca primary beam in the collision with a ^9Be target at energies exceeding 100 MeV/nucleon. The nature of this production mechanism implies that the majority of the produced fragments has fewer neutrons than the projectile. Reactions, however, that involve the removal of several protons with no net loss of neutrons or additional neutrons being picked up from the target nucleus proceed with comparably small cross sections (see for example [1, 2] and references within). The resulting secondary beams of rare isotopes are typically available for experiments at velocities exceeding 30% of the speed of light. A variety of techniques have been developed to enable in-beam spectroscopy studies of fast rare-isotope beams with intensities down to a few atoms per second [3].

Here we report on the in-beam γ -ray spectroscopy of ^{46}S and ^{48}Ar , each produced in a novel way in two steps that both necessarily involve heavy-ion induced nucleon exchange and/or neutron pickup reactions: $^9\text{Be}(^{48}\text{Ca}, ^{48}\text{K})\text{X}$ followed by $^9\text{Be}(^{48}\text{K}, ^{48}\text{Ar}+\gamma)\text{X}$ at 85.7 MeV/u mid-target energy and $^9\text{Be}(^{48}\text{Ca}, ^{46}\text{Cl})\text{X}$ followed by $^9\text{Be}(^{46}\text{Cl}, ^{46}\text{S}+\gamma)\text{X}$ at 87.0 MeV/u mid-target energy, respectively. ^{48}Ar and ^{46}S have neutron number $N = 30$, two neutrons more than the ^{48}Ca primary beam (see Fig. 1). These are the heaviest argon and sulfur isotopes studied with γ -ray spectroscopy to date. As a result, the first excited 2^+ state of ^{46}S was observed for the first time. This is the first time that ^9Be -induced nu-

cleon exchange reactions at intermediate beam energies are used to perform in-beam γ -ray spectroscopy of nuclei more neutron-rich than the projectile.

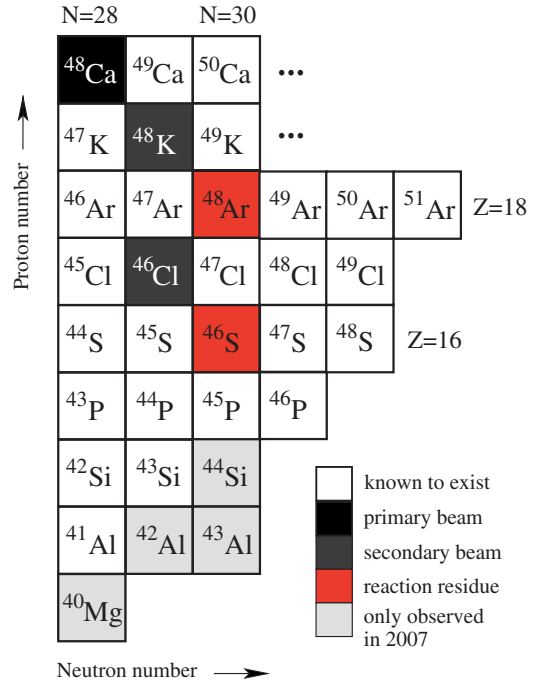


FIG. 1: (Color online) Part of the nuclear chart showing the most neutron-rich nuclei known to exist out to $Z = 18$. Highlighted are ^{48}Ca (primary beam), ^{48}K and ^{46}Cl (secondary beams) and ^{48}Ar and ^{46}S (respective final reaction residues). For comparison, the observation of ^{44}Si [4], ^{40}Mg , ^{42}Al , and possibly ^{43}Al [6] was only achieved in 2007.

The region around ^{42}Si with neutron number $N = 28$ has attracted much attention in recent years. While initial one- and two-proton knockout experiments hinted a proton sub-shell gap at $Z = 14$ [7], inelastic proton scattering in the chain of silicon isotopes [8, 9] and ultimately the observation of the first excited 2^+ state of ^{42}Si at low energy [10] revealed the breakdown of the $N = 28$ shell gap for silicon. Data on the $N = 30$ isotones in this surprising region are scarce. Excited states

in ^{48}Ar have been observed following deep-inelastic reactions [11] while the existence of ^{44}Si has only been proven recently [4]. For ^{46}S , its β -decay half-life [5] had been the only observable accessible to experiments.

Our experiments were performed at the Coupled Cyclotron Facility at NSCL on the campus of Michigan State University. The secondary beams of ^{48}K (pure) and ^{46}Cl (purity exceeding 98%) were produced from a 140 MeV/u stable ^{48}Ca beam impinging on a 705 mg/cm² ^9Be production target and separated using a 390 mg/cm² Al degrader in the A1900 fragment separator [12]. The momentum acceptance of the separator was restricted to 0.5% for the ^{48}K beam and to 2% for the much less intense ^{46}Cl beam, yielding on-target rates of 110×10^3 particles/s and 6×10^3 particles/s, respectively.

The ^9Be reaction target (376 mg/cm² thick) was surrounded by the high-resolution γ -ray detection system SeGA, an array of 32-fold segmented HPGe detectors [13]. The segmentation allows for event-by-event Doppler reconstruction of the γ rays emitted by the reaction residues in flight. The emission angle entering the Doppler reconstruction is determined from the location of the segment with the largest energy deposition. Sixteen detectors were arranged in two rings (90° and 37° central angles with respect to the beam axis). The 37° ring was equipped with seven detectors while nine detectors were located at 90°. The photopeak efficiency of the array was calibrated with standard sources and corrected for the Lorentz boost of the γ -ray distribution emitted by nuclei moving at 39% of the speed of light.

The particle identification was performed event by event with the focal-plane detection system of the large-acceptance S800 spectrograph [14]. The energy loss measured with the S800 ionization chamber and time-of-flight information taken between plastic scintillators – corrected for the angle and momentum of each ion – were used to unambiguously identify the reaction residues emerging from the target. The particle-identification spectrum for ^{48}Ar is shown in Fig. 2 as an example. The most intense constituent in the spectrum is the $^{48}\text{K}^{18+}$ charge state formed by the electron pickup of the initially fully-stripped projectiles in the ^9Be target. Fig. 3(a) and (b) show the longitudinal momentum and the scattering angle distributions of the $^{48}\text{K}^{18+}$ ions passing through the reaction target. The parallel momentum and scattering-angle distributions of ^{48}Ar produced in the reaction $^9\text{Be}(^{48}\text{K}, ^{48}\text{Ar})\text{X}$ are displayed in Fig. 3(c) and (d). The broadening of the momentum distribution and the shift in the maximum of the scattering angle spectrum compared to the $^{48}\text{K}^{18+}$ ions that were not subject of a nuclear reaction (beyond scattering) are clearly visible. However, compared to nucleon removal reactions, the momentum distribution of the nucleon-exchange product is narrow, consistent with the observations by Souliotis *et al.* [1] (for comparison, the measured parallel momentum distribution of ^{47}Ar produced in the one-proton knockout

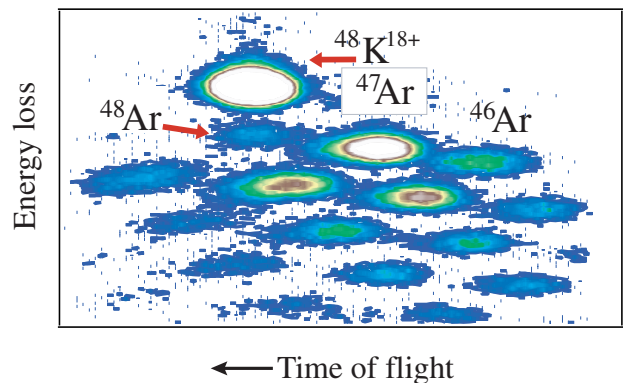


FIG. 2: (Color online) Particle identification spectrum for the reaction residues produced in $^9\text{Be}(^{48}\text{K}, ^{48}\text{Ar})\text{X}$ at 85.7 MeV/u mid-target energy. The energy loss measured in the S800 ionization chamber is plotted versus the ion's time of flight. ^{48}Ar can be unambiguously separated from the projectile-like fragmentation residues produced in the reaction $^{48}\text{K}+^9\text{Be}$.

from ^{48}K under identical conditions – target, projectile end momentum bite – is overlaid).

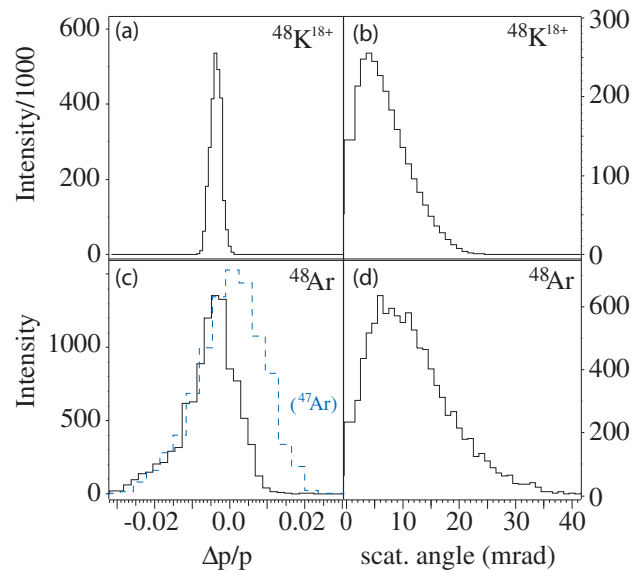


FIG. 3: (Color online) Parallel momentum distribution of the $^{48}\text{K}^{18+}$ ions (a) and the reaction product ^{48}Ar (c) relative to 18.353 GeV/c. (b) and (d) show the reconstructed scattering angle. The $^{48}\text{K}^{18+}$ ions were not subject to a nuclear reaction and the spectra show the effect of the ^9Be -induced nucleon exchange reaction relative to the unreacted $^{48}\text{K}^{18+}$ ions passing through the target. The measured longitudinal momentum distribution of ^{47}Ar produced in the one-proton knockout from ^{48}K under identical conditions is overlaid (blue dashed line).

Inclusive cross sections of $\sigma = 0.13(1)$ mb and $\sigma = 0.057(6)$ mb for the $^9\text{Be}(^{48}\text{K}, ^{48}\text{Ar})\text{X}$ and $^9\text{Be}(^{46}\text{Cl}, ^{46}\text{S})\text{X}$ reactions were derived from the yields of ^{48}Ar and ^{46}S divided by the number of incoming ^{48}K and ^{46}Cl projec-

tiles, respectively, relative to the number density of the reaction target. For each measurement, the normalization of the incoming beam rate was evaluated frequently and a systematic uncertainty of 4% was deduced and added in quadrature to the statistical uncertainty.

The γ -ray spectra observed in coincidence with ^{46}S and ^{48}Ar nuclei – event by event Doppler reconstructed – are displayed in Fig. 4. The γ -ray transition at 952(8) keV in ^{46}S is attributed to the decay of the 2_1^+ state to the 0^+ ground state. This constitutes the first observation of an excited state in this nucleus. Gamma-ray transitions at 1037(6) keV and 1706(10) keV were observed in coincidence with ^{48}Ar and assigned to the $2_1^+ \rightarrow 0_1^+$ and $4_1^+ \rightarrow 2_1^+$ transitions, respectively, in agreement with the results of [11]. Populations of 39(8)% and 34(5)% for the 2^+ and 4^+ states in ^{48}Ar , respectively, were deduced from the efficiency-corrected peak areas, while the remainder is assumed to populate the ground state. In ^{46}S , 63(12)% of the reactions populate the 2_1^+ state. Within our limited statistics, there is no evidence for other γ -ray transitions in the spectrum of ^{46}S .

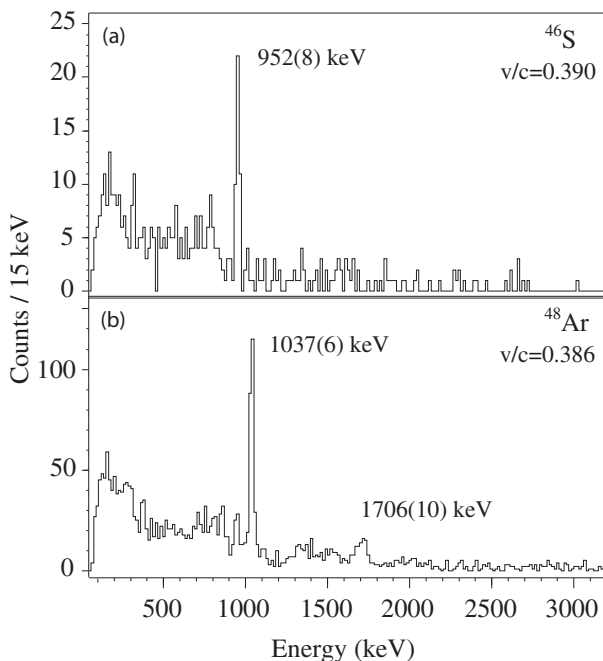


FIG. 4: Event-by-event Doppler reconstructed γ -ray spectra detected in coincidence with ^{46}S and ^{48}Ar . The 952(8) keV peak is attributed to the de-excitation of the 2_1^+ state in ^{46}S . There is no evidence for peaks other than this transition. The two peaks observed at 1037 keV and 1706 keV for ^{48}Ar are attributed to the $2_1^+ \rightarrow 0_1^+$ and $4_1^+ \rightarrow 2_1^+$ transitions, respectively, in agreement with a previous measurement [11].

The energy of the first 2^+ state of ^{46}S we report here constitutes the first measurement of an excited state in a sulfur isotope more neutron-rich than $^{44}\text{S}_{28}$, whose measured collectivity [16] ultimately proved changes to the nuclear structure at neutron number $N = 28$. The con-

sistent description of the onset of collectivity at $N = 28$ in the isotopic chains of sulfur ($Z = 16$) and silicon ($Z = 14$) has been a formidable challenge for shell-model calculations and was achieved only recently by Nowacki and Poves in devising two effective interactions, one for $Z \leq 14$ and one for $Z > 14$ [17].

It is now interesting to track the evolution of the 2_1^+ energies beyond the eroded $N = 28$ magic number in the chains of silicon, sulfur and argon isotopes to probe the dependence of the structure at $N = 30$ on the monopole-shift and pairing modifications that were necessary to describe the silicon isotopes within the shell model.

To study this systematically, shell-model configuration-interaction calculations were carried out in the model space of the sd shell for protons and the pf shell for neutrons starting from the SDFP-NR interaction [15] and introducing a Z -dependent, linear interpolation for pairing and monopole modifications. The experimental energies of the 2_1^+ states (Fig. 5(a)) are compared with those obtained with the SDPF-NR Hamiltonian [15] (Fig. 5(b)). Experiment and theory differ in several ways, in particular for silicon isotopes where the calculated energies are about 400 keV too high for ^{40}Si (and for $^{36,38}\text{Si}$, not shown) and 700 keV too high for ^{42}Si .

Our first modification to SDPF-NR is a reduction of the fp shell $J = 0^+$ matrix element by 0.85 for $Z = 14$. This brings the energy of the 2^+ state in ^{40}Si (and $^{36,38}\text{Si}$, not shown) into better agreement with experiment. The likely reason for this reduction, as discussed in [17], are the reduced proton $2p - 2h$ core-polarization contributions to the effective interaction for silicon compared to calcium, attributed to the larger shell gap for the orbits involved in the case of silicon (i.e., $d_{5/2}$ to $f_{7/2}$) compared to that of calcium (i.e., $d_{3/2}$ to $f_{7/2}$). These core-polarization contributions are likely the reason for the need of two different effective interactions in this region [17]. The results for sulfur and argon in Fig. 5(c) were obtained with a linear interpolation in terms of Z between SDPF-NR (for calcium, $Z = 20$) to SDPF-NR2 (for silicon, $Z = 14$). A similar argument was used to explain the reduction of the sd shell pairing in the carbon isotopes relative to the oxygen isotopes [18].

Our second modification is to reduce the gap between the neutron $f_{7/2}$ and $p_{3/2}$, $p_{1/2}$ orbitals by 1.0 MeV to obtain the interaction SDPF-NR3 for the silicon isotopes. The results obtained with a linear interpolation in terms of Z between SDPF-NR (for calcium) to SDPF-NR3 (for silicon) are shown in Fig. 5(d). A possible reason for the reduction of the shell gap is the lowering of single-particle energies of low- ℓ orbitals ($\ell = 1$) relative to those of high ℓ orbitals ($\ell = 3$) when the energies become small as one approaches the neutron drip line – see Fig. 4 in [19].

The SDPF-NR3 results for 2_1^+ energies of silicon are in good agreement with experiment while the 2_1^+ energies of ^{42}S and ^{44}S obtained with the interpolated interac-

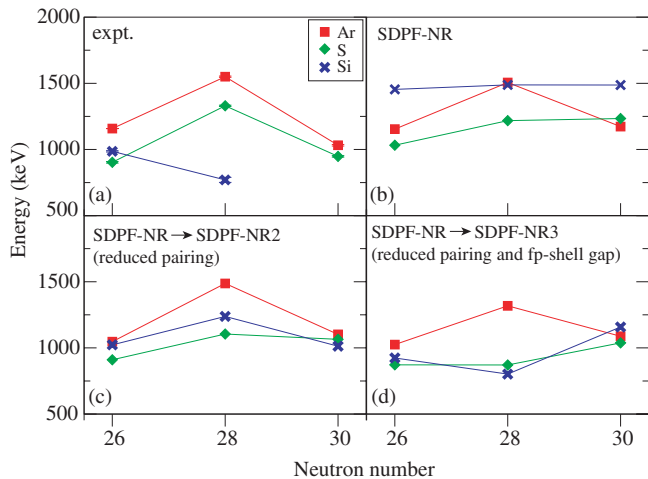


FIG. 5: (Color online) Measured energies of the first 2^+ states in silicon, sulfur and argon isotopes with neutron numbers $N = 26, 28$ and 30 (a) compared to shell-model calculations. The calculation in (b) uses the SDPF-NR effective interaction [15]. The calculations for the silicon isotopes in (c) use the SDPF-NR2 interaction which is derived by reducing the pf shell $J = 0^+$ matrix element by 0.85 . The results for sulfur and argon in (c) are obtained from a linear interpolation in terms of Z between SDPF-NR ($Z = 20$) and SDPF-NR2 ($Z = 14$). The calculations for the silicon isotopes in (d) use the interaction SDPF-NR3 derived by additionally lowering the neutron $p_{3/2}$ and $p_{1/2}$ orbitals by 1 MeV. The results for sulfur and argon in (d) are obtained from a linear interpolation in terms of Z between the SDPF-NR ($Z = 20$) and the SDPF-NR3 ($Z = 14$) interactions.

tions are not. One expects changes in the interaction, but it seems reasonable that they should be smooth as a function of proton and neutron number. In contrast, a linear interpolation between calcium and silicon does not work – and, in accordance with the proposal of [17], the interaction appears to suddenly change at $Z = 14$ also in our approach. The reason for this needs to be understood in terms of a fundamental derivation of the effective interaction for this mass region that takes the effects discussed above into account.

For the $N = 30$ isotones studied experimentally in this work, the original SDPF-NR interaction overestimates the 2_1^+ energies of ^{48}Ar and ^{46}S by 136 keV and 282 keV, respectively. The modifications required for silicon (and implemented for sulfur and argon in terms of an interpolated interaction), only result in a moderate lowering of the calculated 2_1^+ energies of the $N = 30$ isotones, nevertheless reducing the deviation between experiment and calculation SDPF-NR3 to 51 keV and 86 keV for ^{48}Ar and ^{46}S , respectively. This shows that the $N = 30$ isotones are much less impacted by the mechanisms driving the nuclear structure at $N = 28$.

In summary, we used the ^9Be -induced nucleon-exchange reactions $^9\text{Be}(^{48}\text{K}, ^{48}\text{Ar}+\gamma)\text{X}$ and

$^9\text{Be}(^{46}\text{Cl}, ^{46}\text{S}+\gamma)\text{X}$ at above 85 MeV/nucleon mid-target energy for the first time to perform in-beam γ -ray spectroscopy of the $N = 30$ isotones ^{48}Ar and ^{46}S . These heavy-ion induced nucleon-exchange reactions can lead to very exotic nuclei with more neutrons than the projectile beam and thus may be considered a novel approach to reach closer toward the neutron drip line with γ -ray spectroscopy. ^{48}Ar and ^{46}S are the heaviest nuclei of their respective isotopic chains for which γ -ray transitions have been measured; the 2_1^+ state of ^{46}S was established for the first time. The evolution of the 2_1^+ energies for argon, sulfur and silicon isotopes with neutron numbers $N = 26, 28$ and 30 is tracked in comparison to large-scale shell-model calculations using the SDPF-NR effective interaction and Z -dependent interpolations between the original effective interaction and modified versions. Our studies revealed that the description of the $N = 30$ isotones improved, but at much reduced sensitivity, when applying the monopole-shift and pairing corrections required to describe the surprising nuclear structure at $N = 28$. In accordance with the work by Nowacki and Poves – the silicon isotopes emerge as key nuclei with a sudden change occurring in the effective interaction.

This work was supported by the National Science Foundation under Grants No. PHY-0606007 and PHY-0758099.

-
- [1] G. A. Souliotis *et al.*, Phys. Rev. C 46, 1383 (1992).
 - [2] R. Pfaff *et al.*, Phys. Rev. C 51, 1348 (1995).
 - [3] A. Gade and T. Glasmacher, Prog. Part. Nucl. Phys. 60, 161 (2008).
 - [4] O. B. Tarasov *et al.*, Phys. Rev. C 75, 064613 (2007).
 - [5] S. Grévy *et al.*, Phys. Lett. B 594, 252 (2004).
 - [6] T. Baumann *et al.*, Nature 449, 1022 (2007)
 - [7] J. Fridmann *et al.*, Nature 435, 922 (2005); Phys. Rev. C 74, 034313 (2006).
 - [8] C. M. Campbell *et al.*, Phys. Rev. Lett. 97, 112501 (2006).
 - [9] C. M. Campbell *et al.*, Phys. Lett. B 652, 169 (2007).
 - [10] B. Bastin *et al.*, Phys. Rev. Lett. 99, 022503 (2007).
 - [11] A. Bhattacharyya *et al.*, Phys. Rev. Lett. 101, 032501 (2008).
 - [12] D. J. Morrissey *et al.*, Nucl. Instrum. Methods in Phys. Res. B 204, 90 (2003).
 - [13] W. F. Mueller *et al.*, Nucl. Instrum. and Methods in Phys. Res. A 466, 492 (2001).
 - [14] D. Bazin *et al.*, Nucl. Instrum. Methods in Phys. Res. B 204, 629 (2003).
 - [15] S. Nummela *et al.*, Phys. Rev. C 63, 044316 (2001).
 - [16] T. Glasmacher *et al.*, Phys. Lett. B 395, 163 (1997).
 - [17] F. Nowacki and A. Poves, Phys. Rev. C 79, 014310 (2009).
 - [18] M. Stanoiu *et al.*, Phys. Rev. C 78, 034315 (2008).
 - [19] I. Hamamoto, Phys. Rev. C 76, 054319 (2007).